Stem Cell Reports
Resource
OPEN ACCESS

Derivation and FACS-Mediated Purification of PAX3+/PAX7+ Skeletal Muscle Precursors from Human Pluripotent Stem Cells

Bianca Borchin,[1] Joseph Chen,[1] and Tiziano Barberi[1,*]
[1]Australian Regenerative Medicine Institute, Monash University, Clayton, Victoria 3800, Australia
*Correspondence: tb.stemcell.lab@gmail.com
http://dx.doi.org/10.1016/j.stemcr.2013.10.007

SUMMARY

Human pluripotent stem cells (hPSCs) constitute a promising resource for use in cell-based therapies and a valuable in vitro model for studying early human development and disease. Despite significant advancements in the derivation of specific fates from hPSCs, the generation of skeletal muscle remains challenging and is mostly dependent on transgene expression. Here, we describe a method based on the use of a small-molecule GSK3β inhibitor to derive skeletal muscle from several hPSC lines. We show that early GSK3β inhibition is sufficient to create the conditions necessary for highly effective derivation of muscle cells. Moreover, we developed a strategy for stringent fluorescence-activated cell sorting-based purification of emerging PAX3+/PAX7+ muscle precursors that are able to differentiate in postsort cultures into mature myocytes. This transgene-free, efficient protocol provides an essential tool for producing myogenic cells for in vivo preclinical studies, in vitro screenings, and disease modeling.

INTRODUCTION

Pluripotent stem cells (PSCs) such as embryonic stem cells (ESCs) and induced PSCs (iPSCs) provide an extraordinary research tool. In vitro, these cells display extensive proliferation and the ability to differentiate into derivatives of all three germ layers. Such characteristics give these cells a remarkable potential for use in cell-based therapies as well as an in vitro model for early human development. PSC differentiation protocols are currently available for a vast number of cell types (Trounson, 2006); however, little progress has been made regarding differentiation of PSCs into derivatives of paraxial mesoderm, such as skeletal muscle. The difficulty lies in our limited knowledge about specific inductive signals and their timing of expression required for myogenic induction of paraxial mesoderm. The appropriate combination of markers for efficient isolation of skeletal muscle precursors also remains to be determined. As such, only a few studies have reported the derivation of skeletal muscle cells from human PSCs (hPSCs), and they mostly utilized an approach that relies on forced transgene expression to induce myogenesis (Darabi et al., 2012; Goudenege et al., 2012; Ryan et al., 2012). Although a derivation protocol based on the use of genetically modified PSCs can be successful, it does not reflect normal development, does not provide clear information about the identity of the cells generated, and, most importantly, is not suitable for therapeutic purposes or in vitro disease modeling.

We previously reported the generation of specialized, multipotent mesenchymal precursors from hESCs and their directed differentiation into skeletal muscle cells (Barberi et al., 2007). Although that report showed the derivation of skeletal muscle cells from hESCs, the percentage of mesenchymal cells with myogenic potential showed substantial variability. Here, we sought to develop a tightly controlled method to direct hPSCS through defined developmental events leading to the derivation of committed skeletal muscle precursors.

Following a simple two-step differentiation protocol, we first induced paraxial mesoderm by treating hPSCs with a WNT agonist, the small-molecule glycogen synthase kinase-3 inhibitor (CHIR 99021) (Cohen and Goedert, 2004; Tan et al., 2013). In addition to paraxial mesoderm induction, canonical WNT activation acted as a dorsalizing agent, promoting the generation of dorsal neuroepithelial and neural crest cells (Chizhikov and Millen, 2004; Ikeya et al., 1997; Menendez et al., 2011). These cells provide the essential cues for patterning of the paraxial mesoderm and activation of the myogenic program within our cultures (Rios et al., 2011; Tajbakhsh and Buckingham, 2000). Subsequent expansion of the myogenic compartment was achieved through the addition of fibroblast growth factor 2 (FGF2) (Chakkalakal et al., 2012; Lagha et al., 2008).

To isolate skeletal muscle cells generated from our system, we set up a stringent cell-sorting strategy using the muscle-specific nicotinic acetylcholine receptor (AChR) (Karlin, 2002), the chemokine receptor CXCR4 (Buckingham, 2006; Vasyutina et al., 2005), and the hepatocyte growth factor receptor C-MET/HGF (Bladt et al., 1995; Dietrich et al., 1999). Due to their functional roles in hypaxial migratory skeletal muscle, CXCR4 and C-MET allow the isolation of PAX3+ PAX7+ skeletal muscle

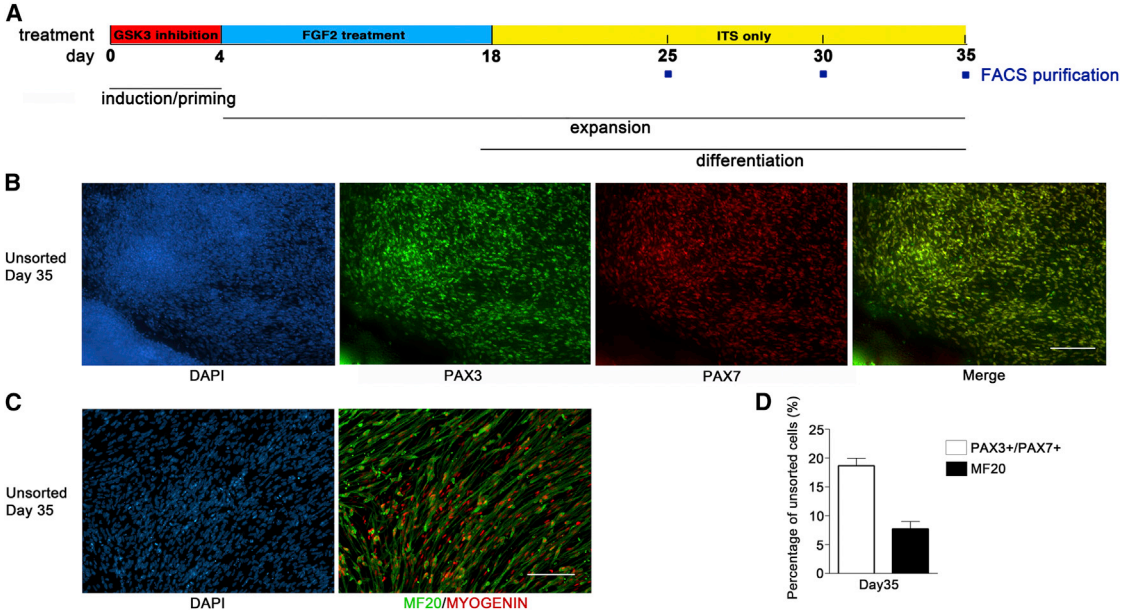

Figure 1. Derivation of Skeletal Muscle from hPSCs

(A) Schematic diagram summarizing the treatment protocol for inducing myogenic differentiation from hPSCs.

(B and C) Immunocytochemical detection of (B) representative fields of PAX3+ and PAX7+ skeletal muscle precursors and (C) MF20+/Myogenin+ mature skeletal myocytes in unsorted cultures at day 35 of hESC (H9) differentiation, under treatment conditions. Scale bar = 50 μm.

(D) Quantitative analysis of PAX3+/7+ nuclei and MF20+ cells at day 35 of hPSC differentiation (H9, HES3, MEL1, and DPL-iPS; n = 4) in unsorted cultures.

Error bars represent the SEM of three or more individual experiments. See also Figure S1.

precursors at high purity (Relaix et al., 2005). Our protocol has been successfully tested on several PSC lines and provides an invaluable standardized tool for the directed derivation of transgene-free myogenic cells for in vivo preclinical studies and for in vitro functional assays and drug screening.

RESULTS

Derivation of Skeletal Muscle Cells from hPSCs

We initiated differentiation of hPSCs at medium to large colony size (diameter 600 μm) and low colony density in serum-free medium consisting of Dulbecco's modified Eagle's medium F-12 (DMEM-F12) supplemented with insulin, transferrin, and selenium (ITS). Paraxial mesoderm specification of hPSCs was achieved through activation of WNT/beta-catenin signaling mediated by the small-molecule GSK-3β inhibitor CHIR 99021 (Cohen and Goedert, 2004; Tan et al., 2013). GSK-3β is known to target a number of substrates for phosphorylation, one of which is beta-catenin, an integral transducer within the canonical WNT signaling pathway. Therefore, inhibition of GSK-3β activity prevents the targeted phosphorylation of beta-catenin, rendering it resistant to degradation and thus leading to activation of T cell factor (TCF)-mediated transcription of downstream target genes (Wu and Pan, 2010). In addition to paraxial mesoderm, WNT signaling is a potent inducer of dorsal cell fates such as roof plate, neural crest, and nonneural ectoderm, marked by LMX1A, SOX10, and AP2α, respectively (Gammill and Bronner-Fraser, 2003; Millonig et al., 2000; Figure S1 available online).

hPSCs were first exposed to 3 μM CHIR for 4 days and then the small molecule was replaced with 20 ng/ml of FGF2 for an additional 2 weeks (Figure 1A). To optimize the differentiation of hPSCs toward a myogenic phenotype, we tested different CHIR concentrations and found high toxicity at >3 μM and inefficient induction at doses of <3 μM (data not shown). The FGF signaling pathway has been identified to regulate several developmental processes of muscle formation. During somitogenesis, segmentation determination is mediated by an FGF signaling gradient within the presomitic mesoderm (Aulehla and Pourquié, 2010). Significantly, FGF molecules such as FGF2 have been described as potent inducers of mitogenic activity in both embryonic skeletal muscle precursors and adult satellite cells (Chakkalakal et al., 2012; Lagha et al.,

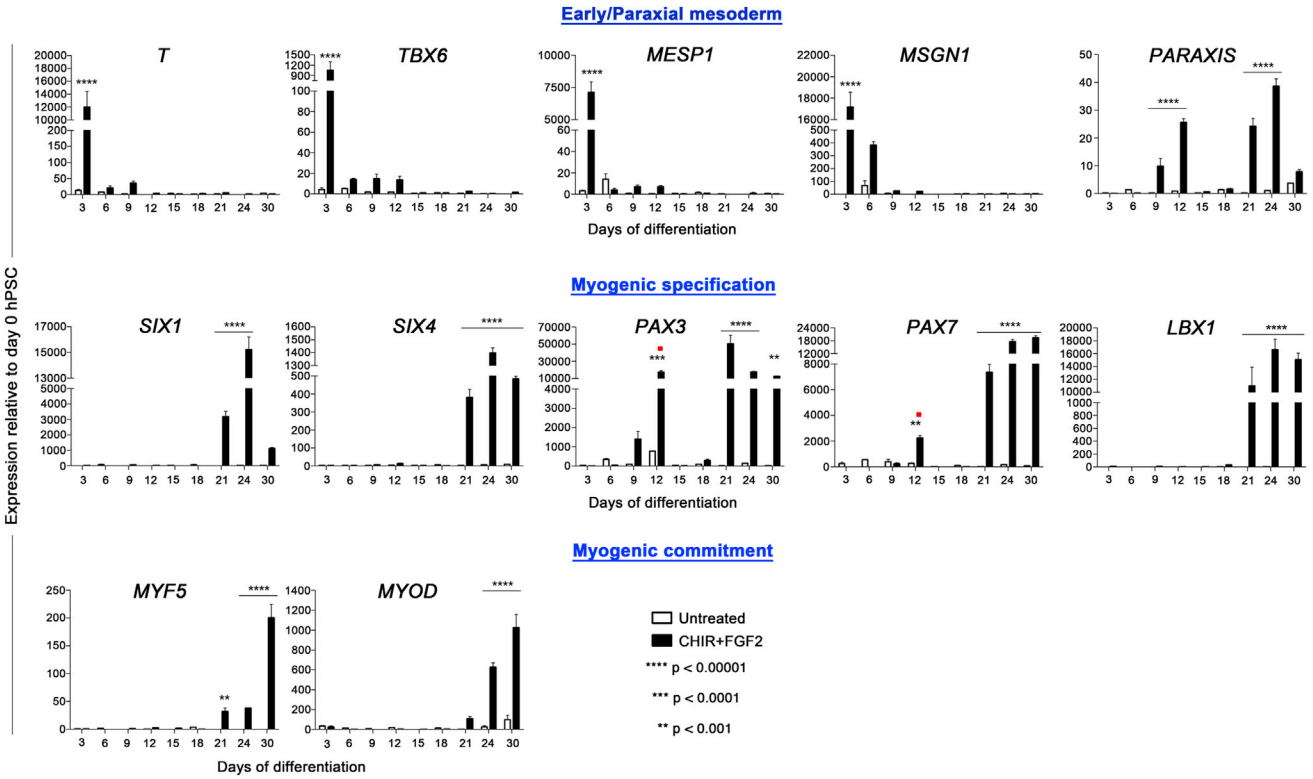

Figure 2. Detection of Gene Transcripts Relevant to the Acquisition of a Myogenic Cell Fate

qPCR analysis showing transcript levels of key muscle development genes from hPSCs (DPL-iPS, H9, MEL1, and HES3; n = 4) differentiating under treatment conditions versus medium alone. Cells were collected and analyzed at 3-day intervals between days 0 and 30 of hPSC differentiation. The relative expression level of each gene is calibrated to its expression at day 0 (represented on the y axis). Cycle threshold (Ct) values for each gene are normalized to the Ct values of the reference gene, *GAPDH*. Values represent mean ± SEM of four independent experiments. Red dots mark early peaks of *PAX3* and *PAX7* expression corresponding to the timing of development of early dorsal neural tissues (roof plate/neural crest). Error bars represent the SEM of three or more individual experiments.

2008). As such, our primary reason for adding FGF2 was to drive expansion of the muscle progenitor compartment within our culture system.

Following withdrawal of FGF2 and a further 17 days of culture in ITS medium alone, areas with skeletal muscle cells were scored in treated culture dishes prior to FACS analysis, and identified by immunocytochemistry as PAX3+ and PAX7+ precursors (Figure 1B; Relaix et al., 2005) and bipolar skeletal myocytes positive for myogenin and sarcomeric myosin (MF20) (Figure 1C). Quantitative analysis revealed the percentage of total PAX3+/PAX7+ and MF20+ muscle cells within the cell culture to be >18% and >8%, respectively, demonstrating the robustness of our treatment strategy.

To further profile the efficacy of our treatment, we analyzed the expression of key regulatory genes associated with the acquisition of a myogenic cell fate by quantitative PCR (qPCR). Data were acquired during a fixed 3-day interval starting at day 0 and ending at day 30 of in vitro differentiation in CHIR+FGF2 compared with untreated hPSCs (Figure 2). Expression profiling of differentiating hPSCs over the course of treatment showed the guided progression of hPSCs through key myogenic milestones. Inhibition of GSK3β resulted in a marked increase in the expression of paraxial/presomitic mesoderm genes such as *TBX6*, *Mesogenin* (*MSGN1*) (Wittler et al., 2007), and *MESP1* (Chan et al., 2013), with an early peak at day 3 of differentiation. Subsequent *PARAXIS* (Burgess et al., 1996) activation starting at day 9 of differentiation indicated progression toward somitic mesoderm. Significantly, expression of the muscle specification genes *SIX1* and *SIX4* (Grifone et al., 2005), *PAX3*, *PAX7*, and the migratory muscle progenitor marker *LBX1* (Gross et al., 2000; Schäfer and Braun, 1999) exhibited marked activation at day 21 of differentiation under the treatment conditions. Expression of the myogenic regulatory factors *MYF5* and *MYOD* indicated muscle commitment and progression of the myogenic differentiation program (Rudnicki et al., 1993).

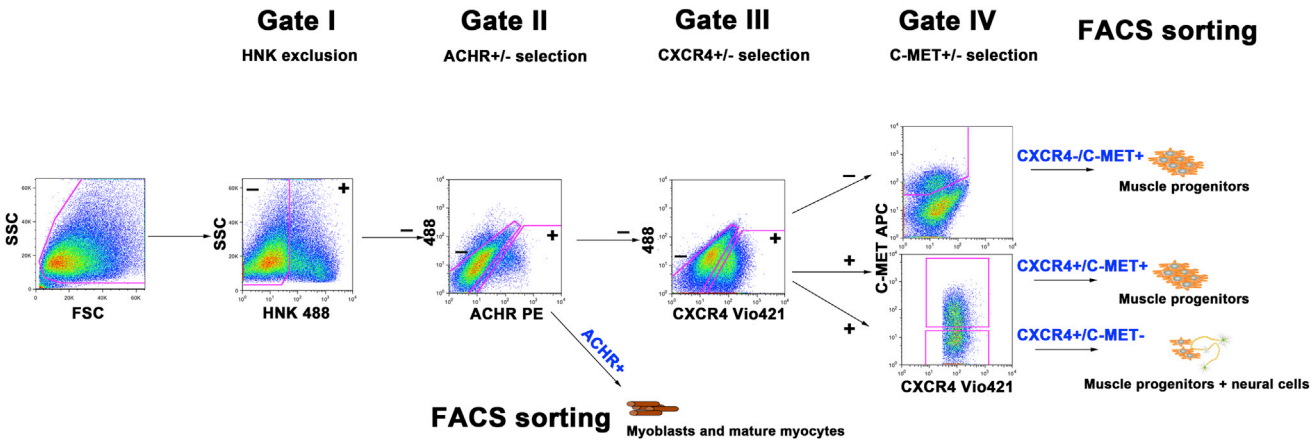

Figure 3. FACS Strategy for the Isolation of Myogenic Cell Populations

Representative experiment in which hESCs (MEL1) that differentiated for 35 days under treatment conditions were sorted based on their HNK, AChR, CXCR4, and C-MET surface marker expression. The gates in each dot plot designate the cell fraction analyzed for the prospective steps; +/− is indicative of either positive or negative expression of each surface antigen. The myogenic cell populations collected from sorting were as follows: (HNK-/AChR+), (HNK−/AChR−/CXCR4−/C-MET+), (HNK−/AChR−/CXCR4+/C-MET+), (HNK−/AChR−/CXCR4+/C-MET−). Gate I: HNK− cells were selected to exclude HNK+ neural/neural crest component. Gate II: selection of HNK−/AChR− cells for myogenic progenitor isolation at subsequent steps or direct isolation of HNK−/AChR+ mature myocytes. Gate III: selection of CXCR4+/− cells. Gate IV: isolation of myogenic progenitor cell populations (HNK−/AChR−/CXCR4−/C-MET+ from gated CXCR4− cells, and HNK−/AChR−/CXCR4+/C-MET+, and HNK−/AChR−/CXCR4+/C-MET−from gated CXCR4+ cells).

In contrast, an insignificant activation of myogenic-specifier genes occurred during differentiation of untreated hPSCs.

Interestingly, *PARAXIS* exhibited a second peak of expression beginning at day 21, correlating with the activation of *SIX1*, *SIX4*, *PAX3*, and *PAX7*. Although it is known to regulate somite epithelization, *Paraxis* has also been shown to be expressed in migratory hypaxial muscle progenitors (Delfini and Duprez, 2000). Therefore, secondary activation of *PARAXIS* expression, in conjunction with expression of *LBX1*, suggests a bias toward hypaxial myogenesis within our system.

FACS Isolation of Hypaxial Skeletal Muscle Precursors

The expression of the migratory skeletal muscle progenitor marker *LBX1* observed in CHIR-treated differentiating hPSCs led us to purify this putative migratory muscle compartment by using CXCR4 and C-MET surface markers, which together are reported to define migratory muscle precursors. Within the hypaxial domain of the embryonic dermomyotome, C-MET expression is critical for the delamination of PAX3+ LBX1+ migratory muscle precursors (Bladt et al., 1995; Dietrich et al., 1999), whereas the subsequent survival and distribution of precursors at the site of migration is CXCR4 dependent (Buckingham, 2006; Vasyutina et al., 2005). However, *CXCR4* and *C-MET* may also be expressed in cells of different origins, such as neural and neural crest cells, respectively (Kos et al., 1999; Zhu and Murakami, 2012). Therefore, to exclude these cell types, we used CD57/HNK-1 as a negative selection marker (Morita et al., 2008). Although CXCR4 can be used to define and isolate definitive endoderm from hPSCs (Teo et al., 2012), the CHIR treatment used in our protocol was not permissive for the generation of endoderm cells, as confirmed by the lack of specific endodermal markers in our cultures (data not shown). Because of the observed activation of myogenic specification genes beginning at day 21 of hPSC differentiation (Figure 2), we isolated skeletal muscle precursors by FACS at three time points (days 25, 30, and 35). The following cell populations were isolated: HNK−/AChR−/CXCR4−/C-MET− (all negative), HNK−/AChR−/CXCR4+/C-MET− (CXCR4+/C-MET−), HNK−/AChR−/CXCR4+/C-MET+ (CXCR4+/C-MET+), and HNK−/AChR−/CXCR4−/C-MET+ (CXCR4−/C-MET+). A detailed gating strategy for the FACS protocol is shown in Figure 3.

Postsorting analysis revealed the presence of myogenic cells only in the populations in which CXCR4 and/or C-MET were present (CXCR4+/C-MET−, CXCR4+/C-MET+, and CXCR4−/C-MET+; Figure 4). To quantify the level of purity in these populations, we performed an immediate postsort immunocytochemical analysis on cytospin preparations. The cytocentrifugation technique spins a cell suspension onto a defined area of a glass slide, creating a monolayer of flattened cells and thus allowing

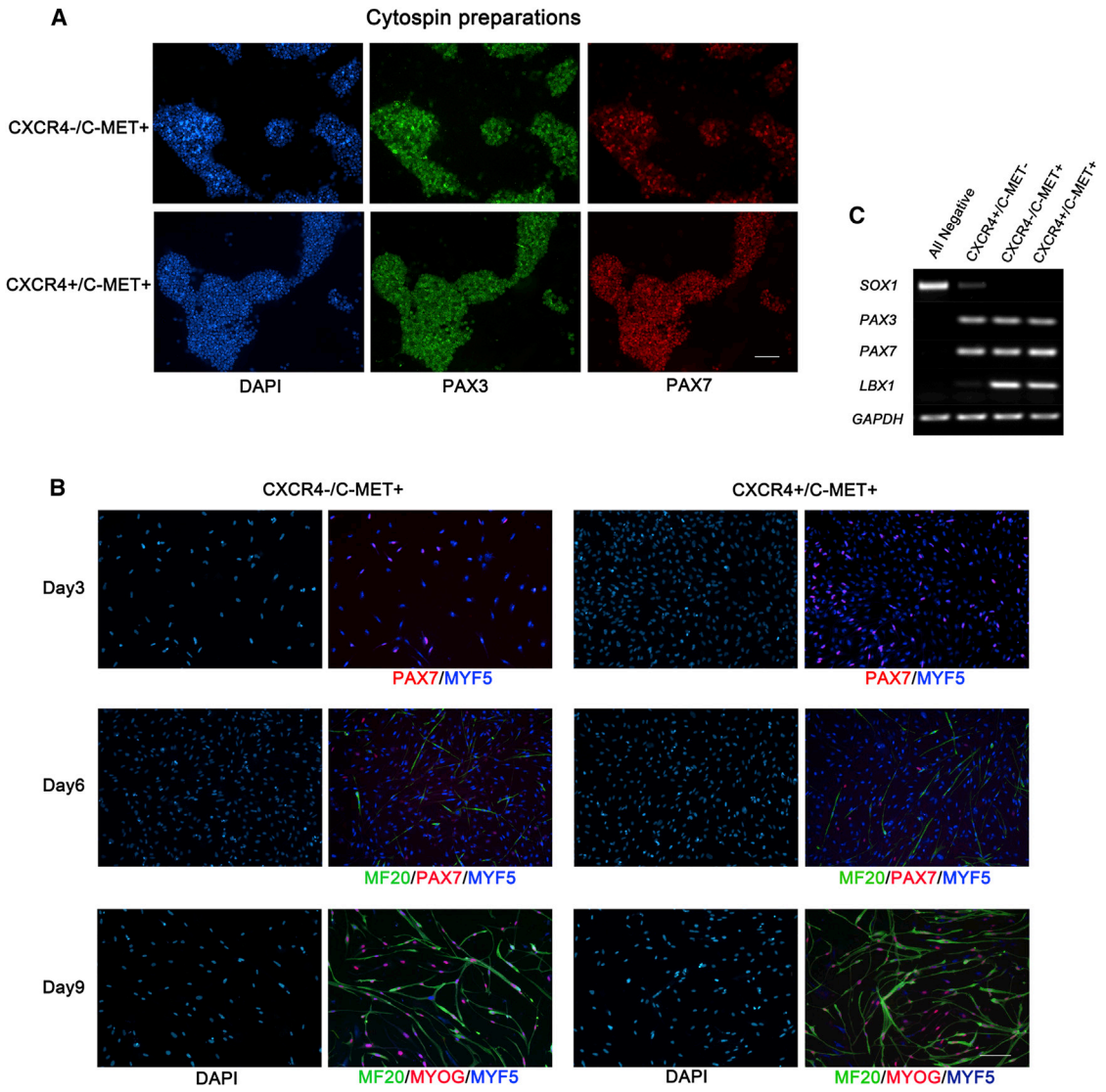

Figure 4. Characterization of CXCR4−/C-MET+ and CXCR4+/C-MET+ Sorted Populations

(A) Cytospin preparations of muscle progenitor cell populations CXCR4−/C-MET+ (top) and CXCR4+/C-MET+ (bottom) sorted at day 35 of hESC (HES3) differentiation. Cells were cytospun on glass slides and analyzed by immunocytochemistry for myogenic stem cell markers PAX3 (green) and PAX7 (red) immediately following sorting. Each dot represents one nucleus as confirmed by DAPI counterstaining.

(B) Immunostaining of replated muscle progenitors CXCR4−/C-MET+ (left) and CXCR4+/C-MET+ (right) (from hESCs [MEL1]) at days 3, 6, and 9 of postsorting cultures shows progression toward a muscle terminal differentiation phenotype.

(C) RT-PCR analysis of skeletal muscle progenitor genes (*PAX3*, *PAX7*, and *LBX1*) and neural gene (*SOX1*) in all sorted populations (from DPL-iPS) derived under treatment conditions. Myog, myogenin; MF20, sarcomeric myosin. Scale bars, 50 μm.

See also Figure S2.

prominent nuclear presentation. Based on nuclear staining, only CXCR4−/C-MET+ and CXCR4+/C-MET+ cell populations allowed the isolation of highly pure skeletal muscle precursors. At day 35, the percentage of total cells immunoreactive for the muscle stem cell marker PAX3 was 97% ± 0.5% in CXCR4−/C-MET+ and 98% ± 0.2% in CXCR4+/C-MET+. The percentage of PAX7 was 84% ± 1.7% in CXCR4−/C-MET+ and 96% ± 2.8% in CXCR4+/C-MET+ (Figure 4A). Immunocytochemical analysis of precursor populations sorted at earlier time points revealed developmental progression of the myogenic program. CXCR4−/C-MET+ and CXCR4+/C-MET+ cells sorted at day 23 were characterized by expression of early myogenic specifier genes SIX4 and PAX3 prior to PAX7 expression. Subsequent acquisition of PAX7 expression, starting at day 25, marked lineage progression (Figure S2). By day

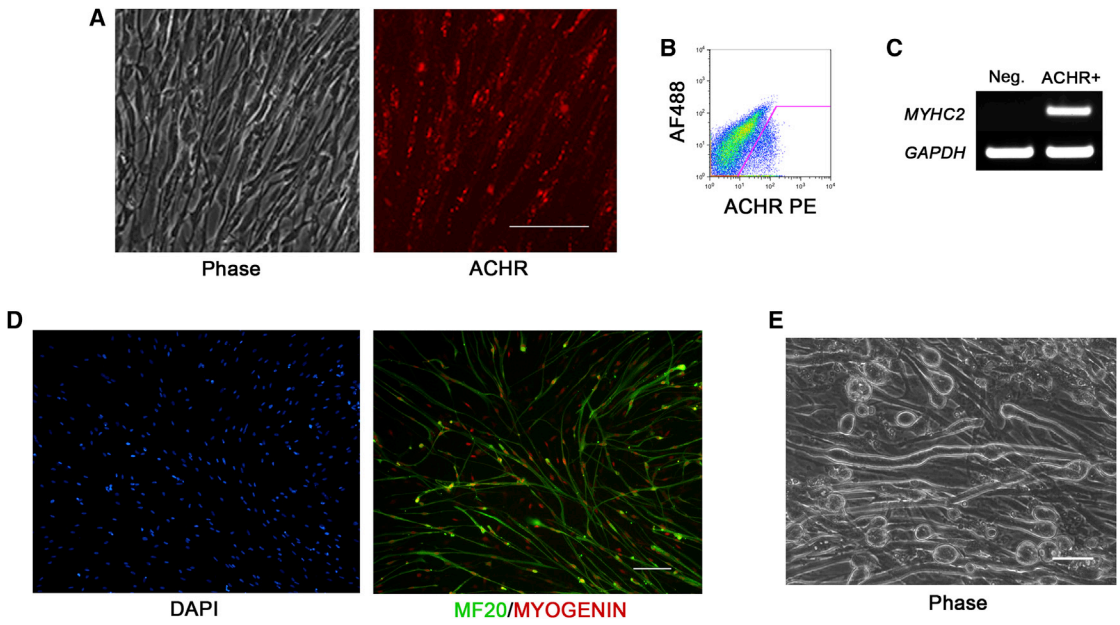

Figure 5. Isolation of AChR+ Skeletal Myocytes

(A) Phase-contrast image (left) and immunocytochemical analysis for AChR expression (right) on hESC-derived (MEL1) skeletal myocytes prior to FACS isolation.

(B) FACS profile of AChR+ cell population (from hESC-H9).

(C) RT-PCR analysis of mature skeletal muscle marker MYH2 in AChR− cells (Neg) and AChR+ cells (from HES3).

(D) Immunocytochemical analysis of hESC-derived AChR+ myocytes (H9) 24 hr postsort, expressing mature skeletal muscle proteins (MF20 and Myog).

(E) Phase-contrast image showing the morphology of AChR+ myocyte-derived myotubes (from H9) after prolonged cell culture (>20 days). Scale bars, 50 μm.

35, close to all CXCR4−/C-MET+ CXCR4+/C-MET+ cells coexpressed PAX3 and PAX7 (Figure 4A). However, an overall lower expression of PAX7 was observed in CXCR4−/C-MET+ cells compared with CXCR4+/C-MET+ cells. Given the earlier activation of *Pax3* (Horst et al., 2006) and the expression of *Cxcr4* in late-stage migratory precursors (Vasyutina et al., 2005) during muscle development, we speculate that CXCR4−/C-MET+ cells could represent a more primitive progenitor population.

Postsorting cultures of CXCR4−/C-MET+ and CXCR4+/C-MET+ cells isolated at day 35 of hPSC differentiation confirmed the validity of the sorting strategy, with all plated cells from both populations undergoing progressive terminal muscle differentiation as shown by expression of MYF5, MYOG, and MF20 (Figure 4B). After 3 days of culture, few cells retained expression of PAX7, whereas all cells expressed MYF5, indicating muscle commitment. By day 9 the majority of cells were in an advanced stage of muscle differentiation.

Gene-expression analysis by RT-PCR confirmed the immunocytochemical data, demonstrating the presence of *PAX3* and *PAX7* mRNA transcripts together with *LBX1* in both CXCR4−/C-MET+ and CXCR4+/C-MET+ sorted populations, and, importantly, their absence in all negative cell populations (Figure 4C).

Although it was enriched in muscle precursors, the CXCR4+/C-MET− cell population showed heterogeneity, with gene-expression analysis revealing the presence of muscle together with SOX1+ neural cells (Figure 4C), and thus would not be useful for in vitro or in vivo studies.

Single-Step FACS Isolation of Mature Skeletal Myocytes

In addition to their potential use in clinical applications, enriched populations of hPSC-derived skeletal muscle cells also provide a platform for basic research investigations. Purification of hPSC-derived mature myocytes offers an unlimited source of cells for large-scale screening of novel therapeutic compounds and toxicity studies. Here, we developed a simple single-antigen strategy for the direct isolation and purification of mature skeletal myocytes.

In our two-step culture system, bipolar skeletal myocytes appeared at approximately 4 weeks of hPSC differentiation. Immunocytochemical analysis revealed strong expression of the muscle-specific nicotinic AChR on these cells (Figure 5A). These receptors are among the first membrane

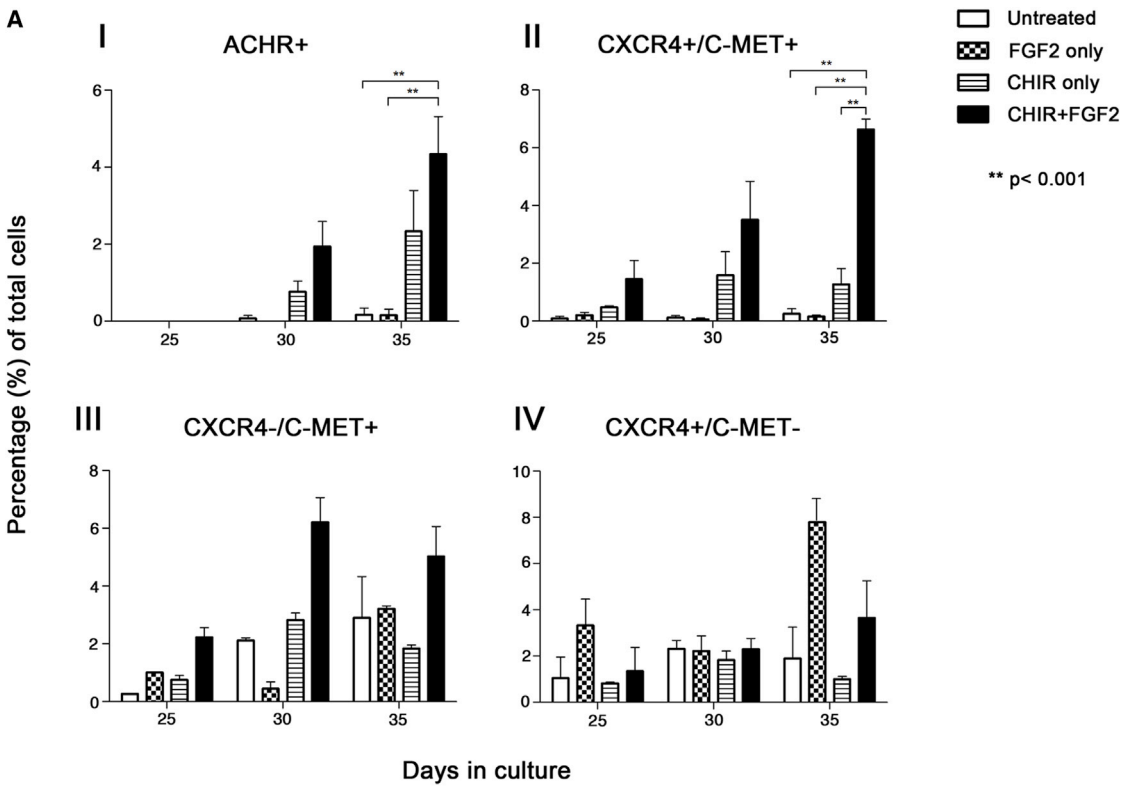

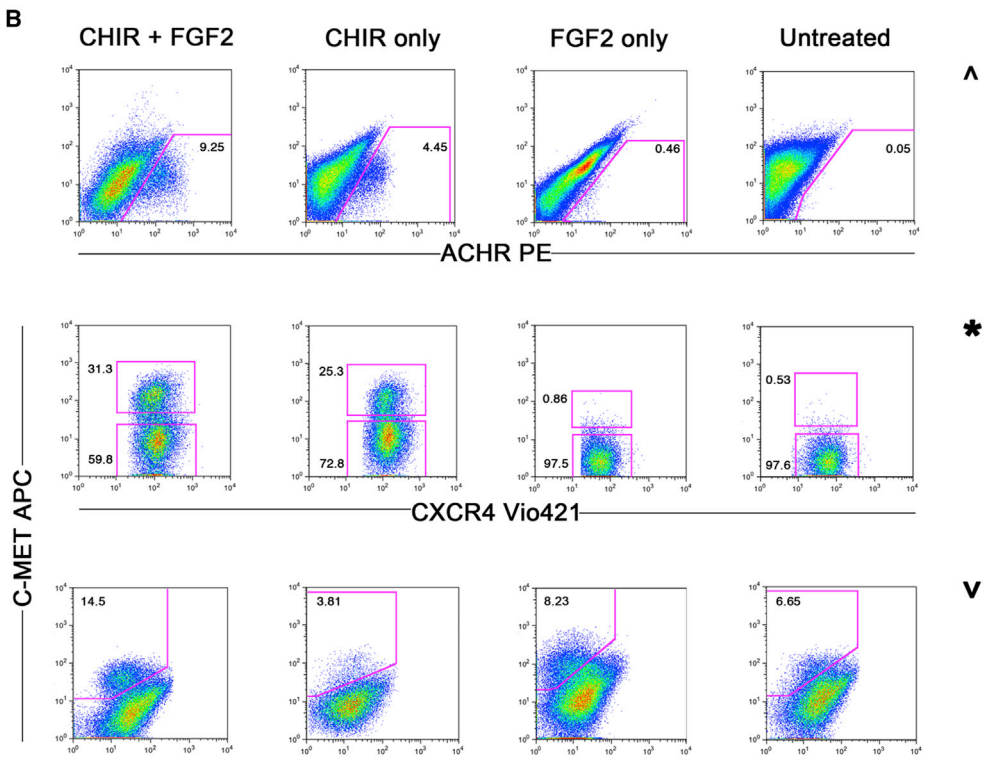

(legend on next page)

proteins to be expressed during skeletal muscle development. However, their presence is required only later during synaptogenesis, when they mediate synaptic transmission at the neuromuscular junction (Brehm and Henderson, 1988). At days 30 and 35 of hPSC differentiation, an easily distinguishable AChR+ population (up to 8% of total cells) was identified and isolated by FACS (Figure 5B). Analysis of both AChR+ and AChR− fractions showed that expression of the mature muscle marker myosin heavy chain 2a (MYHC2) was restricted only to AChR+ cells (Figure 5C).

Following isolation, the AChR+ cells were plated onto fibronectin/laminin-coated plates in the presence of ITS medium. At 24 hr after plating, as expected, all AChR+ cells were immunoreactive for the mature muscle markers myogenin and MF20 (Figure 5D). Prolonged cell culture (>20 days) of AChR+ cells led to the progressive fusion of myocytes into multinucleated myotubes (Figure 5E).

GSK-3 Inhibition Is Required for Efficient Muscle Derivation

We next determined the efficacy of our two-step protocol by comparing four different sorted populations (AChR+, CXCR4+/C-MET+, CXCR4−/C-MET+, and CXCR4+/C-MET−) derived under different culture conditions (CHIR+FGF2, CHIR only, FGF2 only, and untreated). Muscle precursors were already present at day 25 of hPSC differentiation, as indicated by the presence of both CXCR4+/C-MET+ (Figure 6A-II) and CXCR4−/C-MET+ (Figure 6A-III) cell populations. As expected, the overall percentage of each myogenic population increased over time, and thus at day 35, under CHIR+FGF2 treatment, we collectively obtained up to 20% of muscle cells from the AChR+, CXCR4+/C-MET+, and CXCR4−/C-MET+ cell populations (Figures 6A-I, 6A-II, and 6A-III). Significantly, a large component of these cells consisted of PAX3+ and PAX7+ precursors (CXCR4+/C-MET+; CXCR4-/C-MET+), comprising more than 12% of total cells (Figures 6A-II and 6A-III). A similar robust percentage of muscle cells was observed across all four cell lines (three hESCs and one hiPSC), demonstrating the efficiency of our two-step protocol (Figure S3).

CHIR+FGF2 treatment resulted in the efficient derivation of muscle precursors; however, exposure of hPSCs to CHIR only was sufficient for myogenic induction. A reduction in the percentage of CXCR4+/C-MET+ and AChR+ populations compared with CHIR+FGF2 cultures indicated an active role for FGF2 in the expansion of the myogenic compartment (Figures 6A-I, 6A-II, and 6B, top and middle). In stark contrast, the absence of CHIR treatment resulted in almost complete loss of both of these cell fractions (Figures 6A-I, 6A-II, and 6B, top and middle). Interestingly, the overall percentage of CXCR4+/C-MET− and CXCR4−/C-MET+ cells did not change significantly among the four different treatment conditions (Figures 6A-III, 6A-IV, and 6B, middle and bottom). However, a comparative analysis of cell composition among these cell fractions isolated from CHIR+FGF2- or FGF2-only-treated cultures revealed a fundamental shift from a myogenic to a nonmyogenic cell fate in the absence of CHIR treatment (Figure 7). These data illustrate a requirement of CHIR-mediated GSK3β inhibition for the robust induction of muscle cells from hPSCs. The addition of FGF2 is then necessary to achieve optimal expansion of skeletal muscle precursors.

DISCUSSION

The successful use of hPSC-derived progeny for in vitro screening (e.g., for disease modeling, drug development, and toxicity studies) or regenerative medicine requires tight control of the cell differentiation process and isolation of pure, specialized cell types. At present, the controlled derivation and efficient isolation of hPSC-derived myogenic precursors equivalent to in vivo

Figure 6. Quantification of Muscle-Enriched Cell Populations under Four Different Treatment Conditions

AChR+, CXCR4+/C-MET+, CXCR4−/C-MET+, and CXCR4+/C-MET− cell populations derived from hPSCs differentiated under four treatment conditions (CHIR+FGF2, CHIR only, FGF2 only, and untreated) were quantified.

(A) Percentage of AChR+ myocytes (I), CXCR4+/C-MET+ (II) and CXCR4−/C-MET+ (III) precursors, and CXCR4+/C-MET− (IV) mixed population from multiple FACS purification experiments at three different time points. Results shown for each treatment condition represent three experiments averaged from each of the four hPSC lines. (I and II) Fold change difference is observed between CHIR+FGF2 treatment and all other conditions at each time point. CHIR+FGF2 treatment significantly ($p < 0.001$) improves induction of both cell populations at day 35 of differentiation compared with FGF2-only or untreated cultures. (III and IV) The percentage of cells is independent of treatment; however, cell composition is altered (refer to Figure 7).

(B) Representative FACS profile of hPSCs (H9) at day 35 of differentiation. The sorted populations are represented as percentage fractions of the respective parent population. AChR+ (top) and CXCR4+/C-MET+ (middle) cell populations are only present in CHIR-treated hPSCs, whereas CXCR4+/C-MET− (middle) and CXCR4−/C-MET+ (bottom) cell populations are present under all conditions. ^ % of AChR+ gated populations based on HNK− gated fractions; * % of CXCR4+/C-MET+ and CXCR4+/C-MET− gated populations based on HNK−/AChR−/CXCR4+ gated fractions; ˅ % of CXCR4−/C-MET+ gated populations based on HNK−/AChR−/CXCR4− gated fractions.

Error bars represent the SEM of three or more individual experiments. See also Figure S3.

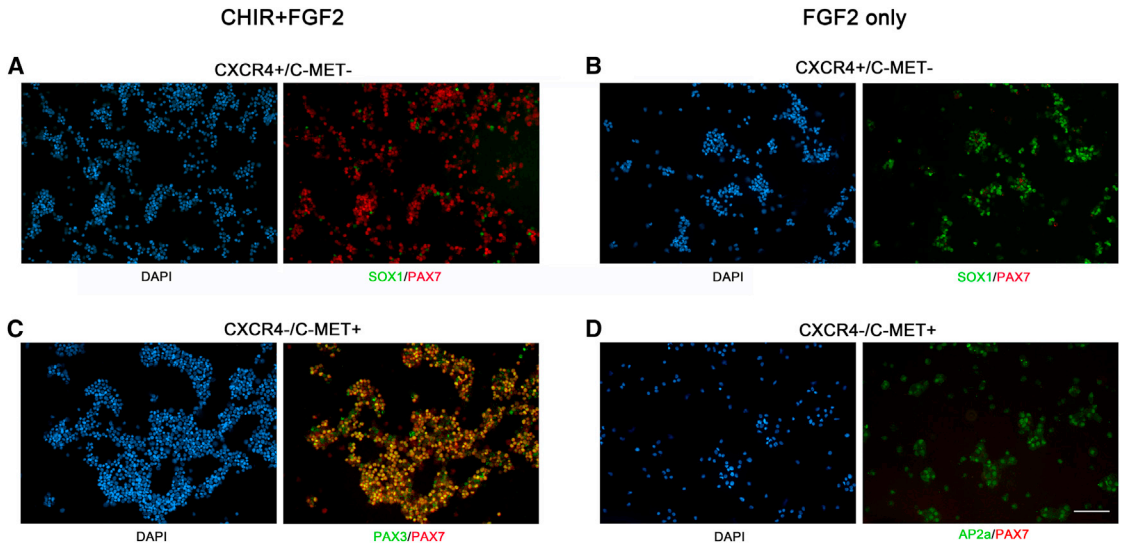

Figure 7. Lack of CHIR Treatment during hPSC Differentiation Results in the Absence of a Muscle Phenotype

(A–D) Immunocytochemical analysis from cytospin preparations of CXCR4+/C-MET− (A and B) and CXCR4−/C-MET+ (C and D) sorted cells.

(A) Under CHIR+FGF2 treatment, the majority of CXCR4+/C-MET− cells are PAX7+, indicating a predominant muscle phenotype.

(B) A complete switch toward SOX1 expression is observed in FGF2-only conditions.

(C) The CXCR4−/C-MET+ cell population derived from CHIR+FGF2-treated hPSCs is composed of highly enriched PAX3+/PAX7+ muscle precursors.

(D) PAX3+ and PAX7+ cells are not present under FGF2-alone conditions, with a large number of cells instead expressing the nonneural ectoderm marker AP2α. Scale bars, 50 μm. All images from hESC HES3.

PAX3+/PAX7+ satellite cells has not been accomplished. Attempts to derive such cells are hindered by our lack of knowledge about the essential factors required in vitro to recapitulate the in vivo patterning of myogenic somitic mesoderm and the timing of their distribution. This may explain the limited success to date and the large number of published protocols that rely on an artificial system of derivation utilizing forced transgene expression (Darabi et al., 2012; Goudenege et al., 2012). Although Ryan et al. (2012) recently provided evidence of muscle differentiation from hESCs without genetic modification, their approach was hindered by the use of serum in the medium, low myogenic induction, and fundamentally the lack of any purification strategy.

Here, we present a simple, two-step differentiation method that recapitulates the early events of embryogenesis to efficiently derive PAX3+/PAX7+ skeletal muscle precursors from hPSCs. We demonstrate the feasibility of deriving robust numbers of skeletal muscle cells without the aid of transgene-driven differentiation.

Central to this method is the activation of canonical WNT signaling by the GSK3β inhibitor CHIR. Expression profiling of hPSCs over the course of guided differentiation showed progression through defined developmental milestones leading to myogenesis. This transition was initiated by a strong induction of *TBX6*, *MESP1*, and *MSGN1* in CHIR-treated hPSCs, followed by high levels of *PARAXIS* expression, indicating progression into somitic mesoderm. In addition to the induction of paraxial mesoderm, activation of WNT signaling by CHIR was responsible for generating dorsal tissues, such as dorsal neural tube cells marked by LMX1A expression, along with SOX10+ neural crest cells and AP2α+ nonneural ectoderm (Figure S1). It has been established that myogenic patterning of the dermomyotome requires WNT signaling from the dorsal neural tube and overlying ectoderm (Tajbakhsh and Buckingham, 2000), together with transient, neural-crest-mediated notch activation of myogenic precursors (Rios et al., 2011). Early GSK3β inhibition during hPSC differentiation allowed us to reproduce the conditions necessary for the specification of skeletal muscle cells, closely replicating the events that occur during normal development in vivo. We speculate that the generation of dorsal tissues played an essential role in delivering the appropriate signals required for the patterning of the presomitic mesoderm within our culture system. Conversely, prolonged exposure to CHIR for up to 10 days was shown to have a negative effect on muscle derivation, and no muscle cells were identified in the treated dishes (data not shown). Although we show that CHIR alone is sufficient for myogenic induction, prolonged FGF2 exposure proved to play a proliferative role

by significantly increasing the number of myogenic precursors.

We validated the robustness of our protocol by obtaining similar results with four hPSC lines, confirming that small-molecule-mediated GSK3β inhibition is a simple but highly efficient approach for directing the differentiation of hPSCs into skeletal muscle precursors.

Progress in considering hPSC-derived muscle as a valid source of cells for basic and translational research applications has been hindered by the lack of an efficient method to isolate muscle precursors. To overcome this limitation, we developed a FACS strategy to purify muscle precursors generated in our differentiation system. Since we detected *LBX1* transcripts during directed myogenic commitment of hPSCs, we considered the use of two markers that are known to be highly expressed in hypaxial migratory muscle precursors during development: C-MET and CXCR4. FACS selection of two populations, CXCR4−/C-MET+ and CXCR4+/C-MET+, allowed the isolation of PAX3+/PAX7+ precursors at high purity. Notably, the negative cell population (HNK−/AChR−/CXCR4−/C-MET−) was devoid of any muscle markers, indicating not only that our sorting strategy is sufficient to isolate all skeletal muscle cells generated in our culture system but also that all PAX3+/PAX7+ precursors are of hypaxial origin. The specificity of this strategy is also confirmed by the complete absence of CXCR4+/C-MET+ cells and by a nonmuscle identity of CXCR4-/C-MET+ cells in the absence of early GSK3β inhibition during hPSC differentiation.

Transplantation of highly purified skeletal muscle precursors has been considered a possible option for the treatment of degenerative muscle disorders, such as muscular dystrophy. Our findings will accelerate the evaluation of the therapeutic potential of hPSC-derived muscle cells in preclinical models. Moreover, future applications of our method to patient-specific iPSC lines will aid in the study of muscle development during disease.

In addition to the isolation of skeletal muscle precursors, we described a simple strategy for the direct isolation of mature skeletal myocytes through the positive selection of AChR+ cells. This highly efficient derivation and direct isolation of mature embryonic stage skeletal myocytes provides a platform for developmental modeling and candidate drug screening.

In conclusion, we have developed a small-molecule-based approach and identified GSK3β inhibition as a requirement for the efficient, nongenetic derivation of skeletal muscle cells from hPSCs. Our cell-sorting strategy based on the use of functional markers allows the purification of hPSC-derived PAX3+/PAX7+ skeletal muscle precursors. This work describes the derivation and isolation of early muscle precursors with a defined phenotype.

EXPERIMENTAL PROCEDURES

Culture of Undifferentiated hPSCs

hPSC lines (WA-09 [H9], Mel1, HES3, and PDL-iPS), passages p40–65, were maintained on hESC-qualified Matrix (BDMatrigel; BD Biosciences) in the presence of mTESR1 medium (Stem Cell Technologies) as previously described (Ludwig and Thomson, 2007). The experiments performed with hESCs in this study were approved by the Monash University Human Research Ethics Committee (CF09/2725).

Directed Differentiation of hPSCs into Skeletal Muscle Cells

Experiments were performed with all four hPSC lines. When the colony size reached >600 μm in diameter and the colony density on the plate was approximately 30%–40%, we induced differentiation of hPSC by switching the culture medium from mTESR1 to a chemically defined, serum-free medium, DMEM-F12, supplemented with ITS (all from Sigma-Aldrich). Starting at day 0 of differentiation, cells were cultured in the presence of 3 μM CHIR 99021 (Miltenyi Biotech) for 4 days. The culture medium was then replaced by ITS containing 20 ng/ml of FGF2 (Miltenyi Biotech) for a further 14 days. For each experimental control condition, hPSC differentiation was induced by (1) CHIR only (ITS medium containing 3 μM CHIR from days 0 to 4, followed by ITS medium only until the day of analysis) or (2) FGF2 only (ITS medium only between days 0 and 4, followed by ITS medium containing 20 ng/ml FGF2 for 14 days). The medium was replaced daily until the day of analysis.

FACS

Cells were dissociated with 0.05% trypsin or TrypLE Select (Invitrogen) to a single-cell suspension and incubated with the appropriate fluorochrome-labeled antibodies (Table S2) at a concentration of 10^7 cells/ml for 30 min on ice. Indirect labeling of HNK and AChR antibodies was done using goat anti-mouse Alexa Fluor 488 and goat anti-mouse PE (both from Molecular Probes/Invitrogen) as secondary antibodies. Labeled cells were sorted through a BD Influx (five lasers) flow sorter (BD Biosciences) according to the excitation requirements of the fluorochromes. Sorted populations were analyzed using FlowJo software (Tree Star).

Immunocytochemistry

For cytospin preparations of FACS-sorted populations, cells were spun onto glass slides using Cytospin 4 (Shandon; Thermofisher). Cells were then fixed with 100% cold methanol for 5 min and subsequently rehydrated in PBS for 15–20 min. The cultured cells were fixed with 4% paraformaldehyde for 10 min at room temperature and permeabilized with 0.3% Triton X-100 in PBS for 30 min. A complete list of the primary and fluorochrome-labeled secondary antibodies used in this study is provided in Table S2. Incubations with primary and subsequently secondary antibodies were performed in incubation buffer (0.1% BSA, 2% fetal bovine serum [FBS], 0.1% Triton X-100 in PBS) for 40 min at 37°C. Image acquisition was performed on an inverted Nikon Eclipse Ti epifluorescence microscope with

the appropriate filter sets using single-channel acquisition on a Nikon Digital sight DS-U2 camera. Images were analyzed with Nikon NIS-Elements 3.2 software. All immunofluorescence images are representative of one individual experiment. Three experiments per cell line were performed. Similar results were obtained in all cell lines.

Gene-Expression Analysis

Total RNA was extracted using the RNeasy Mini kit (QIAGEN), and DNase I treatment (QIAGEN) was performed to avoid genomic DNA contamination. The Ambion RETROscript First Strand Synthesis Kit (Invitrogen) was used to reverse transcribe total RNA (500 ng each sample). PCR was performed using the Mastercyler proS (Eppendorf AG). We optimized the PCR conditions and determined the linear amplification range for each primer by varying the annealing temperature and cycle number. Primer sequences, cycle numbers, and annealing temperatures are provided in Table S1. All RT-PCR data shown are representative of one individual experiment. Three experiments per cell line were performed. Similar results were obtained in all cell lines.

For qPCR, *GAPDH* was used as a reference gene and reactions were run using LightCycler480 SYBR Green I Master (Roche Applied Science) on a LightCycler 480 system (Roche Applied Science). Target gene expression was normalized to the reference gene (*GAPDH*), and subsequent quantification of gene expression was compared relative to day 0 undifferentiated hPSCs (Pfaffl, 2001).

Culture of FACS-Isolated Cell Populations

FACS-purified AChR+ myocytes and CXCR4−/C-MET+ and CXCR4+/C-MET+ precursors were plated onto tissue culture wells coated with 2 μg/ml fibronectin and 2 μg/ml laminin (both from Invitrogen) in ITS medium supplemented with 10 μM Rock Inhibitor Y-27632 (Sigma Aldrich). Myocytes were maintained in ITS medium in the presence of 50 ng/ml IGF1 (Peprotech) until they were analyzed. Progenitor cell populations were cultured in ITS medium until terminal muscle differentiation occurred.

Statistical Analysis

Data were analyzed by two-way ANOVA followed by Bonferroni's post test to calculate p values. Analyses were performed using statistical software (GraphPad Prism 5.04; GraphPad Software). Probability values < 0.05 were considered statistically significant. Error bars in each figure represent the SEM of three or more individual experiments. For qPCR data, p values were calculated for changes in expression of markers over time compared with day 0. For quantitative analysis of FACS sorting data, the percentage of myogenic cells relative to the total number of cells was obtained for each experimental culture treatment, and p values were calculated for differences between the means of each experimental condition.

SUPPLEMENTAL INFORMATION

Supplemental Information includes three figures and two tables and can be found with this article online at http://dx.doi.org/10.1016/j.stemcr.2013.10.007.

ACKNOWLEDGMENTS

We thank Dr. Rodica Stan and Dr. Joly Kwek for critical readings of the manuscript. We thank Dr. Andrew Laslett for providing the iPSC line PDL-iPS. The Australian Regenerative Medicine Institute is supported by grants from the State Government of Victoria and the Australian Government. B.B. is supported by an Australian Rotary Health PhD scholarship.

Received: August 16, 2013
Revised: October 15, 2013
Accepted: October 16, 2013
Published: November 27, 2013

REFERENCES

Aulehla, A., and Pourquié, O. (2010). Signaling gradients during paraxial mesoderm development. Cold Spring Harb. Perspect. Biol. *2*, a000869.

Barberi, T., Bradbury, M., Dincer, Z., Panagiotakos, G., Socci, N.D., and Studer, L. (2007). Derivation of engraftable skeletal myoblasts from human embryonic stem cells. Nat. Med. *13*, 642–648.

Bladt, F., Riethmacher, D., Isenmann, S., Aguzzi, A., and Birchmeier, C. (1995). Essential role for the c-met receptor in the migration of myogenic precursor cells into the limb bud. Nature *376*, 768–771.

Brehm, P., and Henderson, L. (1988). Regulation of acetylcholine receptor channel function during development of skeletal muscle. Dev. Biol. *129*, 1–11.

Buckingham, M. (2006). Myogenic progenitor cells and skeletal myogenesis in vertebrates. Curr. Opin. Genet. Dev. *16*, 525–532.

Burgess, R., Rawls, A., Brown, D., Bradley, A., and Olson, E.N. (1996). Requirement of the paraxis gene for somite formation and musculoskeletal patterning. Nature *384*, 570–573.

Chakkalakal, J.V., Jones, K.M., Basson, M.A., and Brack, A.S. (2012). The aged niche disrupts muscle stem cell quiescence. Nature *490*, 355–360.

Chan, S.S., Shi, X., Toyama, A., Arpke, R.W., Dandapat, A., Iacovino, M., Kang, J., Le, G., Hagen, H.R., Garry, D.J., and Kyba, M. (2013). Mesp1 patterns mesoderm into cardiac, hematopoietic, or skeletal myogenic progenitors in a context-dependent manner. Cell Stem Cell *12*, 587–601.

Chizhikov, V.V., and Millen, K.J. (2004). Mechanisms of roof plate formation in the vertebrate CNS. Nat. Rev. Neurosci. *5*, 808–812.

Cohen, P., and Goedert, M. (2004). GSK3 inhibitors: development and therapeutic potential. Nat. Rev. Drug Discov. *3*, 479–487.

Darabi, R., Arpke, R.W., Irion, S., Dimos, J.T., Grskovic, M., Kyba, M., and Perlingeiro, R.C. (2012). Human ES- and iPS-derived myogenic progenitors restore DYSTROPHIN and improve contractility upon transplantation in dystrophic mice. Cell Stem Cell *10*, 610–619.

Delfini, M.C., and Duprez, D. (2000). Paraxis is expressed in myoblasts during their migration and proliferation in the chick limb bud. Mech. Dev. *96*, 247–251.

Dietrich, S., Abou-Rebyeh, F., Brohmann, H., Bladt, F., Sonnenberg-Riethmacher, E., Yamaai, T., Lumsden, A., Brand-Saberi, B., and

Birchmeier, C. (1999). The role of SF/HGF and c-Met in the development of skeletal muscle. Development *126*, 1621–1629.

Gammill, L.S., and Bronner-Fraser, M. (2003). Neural crest specification: migrating into genomics. Nat. Rev. Neurosci. *4*, 795–805.

Goudenege, S., Lebel, C., Huot, N.B., Dufour, C., Fujii, I., Gekas, J., Rousseau, J., and Tremblay, J.P. (2012). Myoblasts derived from normal hESCs and dystrophic hiPSCs efficiently fuse with existing muscle fibers following transplantation. Mol. Ther. *20*, 2153–2167.

Grifone, R., Demignon, J., Houbron, C., Souil, E., Niro, C., Seller, M.J., Hamard, G., and Maire, P. (2005). Six1 and Six4 homeoproteins are required for Pax3 and Mrf expression during myogenesis in the mouse embryo. Development *132*, 2235–2249.

Gross, M.K., Moran-Rivard, L., Velasquez, T., Nakatsu, M.N., Jagla, K., and Goulding, M. (2000). Lbx1 is required for muscle precursor migration along a lateral pathway into the limb. Development *127*, 413–424.

Horst, D., Ustanina, S., Sergi, C., Mikuz, G., Juergens, H., Braun, T., and Vorobyov, E. (2006). Comparative expression analysis of Pax3 and Pax7 during mouse myogenesis. Int. J. Dev. Biol. *50*, 47–54.

Ikeya, M., Lee, S.M., Johnson, J.E., McMahon, A.P., and Takada, S. (1997). Wnt signalling required for expansion of neural crest and CNS progenitors. Nature *389*, 966–970.

Karlin, A. (2002). Emerging structure of the nicotinic acetylcholine receptors. Nat. Rev. Neurosci. *3*, 102–114.

Kos, L., Aronzon, A., Takayama, H., Maina, F., Ponzetto, C., Merlino, G., and Pavan, W. (1999). Hepatocyte growth factor/scatter factor-MET signaling in neural crest-derived melanocyte development. Pigment Cell Res. *12*, 13–21.

Lagha, M., Kormish, J.D., Rocancourt, D., Manceau, M., Epstein, J.A., Zaret, K.S., Relaix, F., and Buckingham, M.E. (2008). Pax3 regulation of FGF signaling affects the progression of embryonic progenitor cells into the myogenic program. Genes Dev. *22*, 1828–1837.

Ludwig, T., and Thomson, J.A. (2007). Defined, feeder-independent medium for human embryonic stem cell culture. Curr. Protoc. Stem Cell Biol. *2*, 1C.2.1–1C.2.16.

Menendez, L., Yatskievych, T.A., Antin, P.B., and Dalton, S. (2011). Wnt signaling and a Smad pathway blockade direct the differentiation of human pluripotent stem cells to multipotent neural crest cells. Proc. Natl. Acad. Sci. USA *108*, 19240–19245.

Millonig, J.H., Millen, K.J., and Hatten, M.E. (2000). The mouse Dreher gene Lmx1a controls formation of the roof plate in the vertebrate CNS. Nature *403*, 764–769.

Morita, I., Kizuka, Y., Kakuda, S., and Oka, S. (2008). Expression and function of the HNK-1 carbohydrate. J. Biochem. *143*, 719–724.

Pfaffl, M.W. (2001). A new mathematical model for relative quantification in real-time RT-PCR. Nucleic Acids Res. *29*, e45.

Relaix, F., Rocancourt, D., Mansouri, A., and Buckingham, M. (2005). A Pax3/Pax7-dependent population of skeletal muscle progenitor cells. Nature *435*, 948–953.

Rios, A.C., Serralbo, O., Salgado, D., and Marcelle, C. (2011). Neural crest regulates myogenesis through the transient activation of NOTCH. Nature *473*, 532–535.

Rudnicki, M.A., Schnegelsberg, P.N., Stead, R.H., Braun, T., Arnold, H.H., and Jaenisch, R. (1993). MyoD or Myf-5 is required for the formation of skeletal muscle. Cell *75*, 1351–1359.

Ryan, T., Liu, J., Chu, A., Wang, L., Blais, A., and Skerjanc, I.S. (2012). Retinoic acid enhances skeletal myogenesis in human embryonic stem cells by expanding the premyogenic progenitor population. Stem Cell Rev. *8*, 482–493.

Schäfer, K., and Braun, T. (1999). Early specification of limb muscle precursor cells by the homeobox gene Lbx1h. Nat. Genet. *23*, 213–216.

Tajbakhsh, S., and Buckingham, M. (2000). The birth of muscle progenitor cells in the mouse: spatiotemporal considerations. Curr. Top. Dev. Biol. *48*, 225–268.

Tan, J.Y., Sriram, G., Rufaihah, A.J., Neoh, K.G., and Cao, T. (2013). Efficient derivation of lateral plate and paraxial mesoderm subtypes from human embryonic stem cells through GSKi-mediated differentiation. Stem Cells Dev. *22*, 1893–1906.

Teo, A.K., Ali, Y., Wong, K.Y., Chipperfield, H., Sadasivam, A., Poobalan, Y., Tan, E.K., Wang, S.T., Abraham, S., Tsuneyoshi, N., et al. (2012). Activin and BMP4 synergistically promote formation of definitive endoderm in human embryonic stem cells. Stem Cells *30*, 631–642.

Trounson, A. (2006). The production and directed differentiation of human embryonic stem cells. Endocr. Rev. *27*, 208–219.

Vasyutina, E., Stebler, J., Brand-Saberi, B., Schulz, S., Raz, E., and Birchmeier, C. (2005). CXCR4 and Gab1 cooperate to control the development of migrating muscle progenitor cells. Genes Dev. *19*, 2187–2198.

Wittler, L., Shin, E.H., Grote, P., Kispert, A., Beckers, A., Gossler, A., Werber, M., and Herrmann, B.G. (2007). Expression of Msgn1 in the presomitic mesoderm is controlled by synergism of WNT signalling and Tbx6. EMBO Rep. *8*, 784–789.

Wu, D., and Pan, W. (2010). GSK3: a multifaceted kinase in Wnt signaling. Trends Biochem. Sci. *35*, 161–168.

Zhu, Y., and Murakami, F. (2012). Chemokine CXCL12 and its receptors in the developing central nervous system: emerging themes and future perspectives. Dev. Neurobiol. *72*, 1349–1362.